



Cite this: *Environ. Sci.: Adv.*, 2025, 4, 1191

Received 19th April 2025
Accepted 1st July 2025

DOI: 10.1039/d5va00106d

rsc.li/esadvances

Unique adaptations of a photosynthetic microbe *Rhodopseudomonas palustris* to the toxicological effects of perfluorooctanoic acid†

Mark Kathol,‡^a Anika Azme,‡^b Sumaiya Saifur,^c Nirupam Aich,^d *^b and Rajib Saha,^d *^a

In this study, we investigate the PFOA removal capabilities of *Rhodopseudomonas palustris* (*R. palustris*), a fluoroacetate dehalogenase containing microbe, as a potential candidate for achieving bioremediation. In the 50-day PFOA uptake experiment, *R. palustris* removed $44 \pm 6.34\%$ PFOA after 20 days of incubation, which was then reduced to a final removal of $6.23 \pm 12.75\%$. Results indicate that PFOA was temporarily incorporated into the cell membrane before being partially released into the media after cell lysis. This incorporation might be attributed to the combined effect of the hydrophobic interaction between PFOA and the cell membrane and the reduced electrostatic repulsion from the high ion concentration in the growth medium. The growth of *R. palustris* during the PFOA uptake experiment was 45-fold slower than their growth without PFOA. This study also completely defines the toxicity range of PFOA for *R. palustris* through a toxicity assay. Increasing PFOA concentration reduced microbial growth, with complete inhibition observed at around 200 ppm. An accelerated growth phase was followed by a temporary death phase in the first 24 hours in the presence of 12.5–100 ppm PFOA, implying a unique adaptation mechanism to PFOA.

Environmental significance

Widespread PFAS contamination in different water matrices is one of the current critical challenges. Contemporary treatment technologies struggle to effectively remove these compounds, necessitating the exploration of alternative remediation strategies. *Rhodopseudomonas palustris* CGA009 (*R. palustris*) is a promising candidate for bioremediation avenues due to its ability to consume recalcitrant carbon feedstocks and possession of a fluoroacetate dehalogenase enzyme. Here, we showcase that this microbe can remove perfluorooctanoic acid (PFOA) molecules from water by incorporating them into the cells. In the presence of high PFOA concentration, these microbes survive by uniquely adapting their growth pattern. Understanding the mechanisms underlying *R. palustris* interactions with PFOA might pave the way for similar microbial-based treatment technologies that mitigate PFAS from contaminated environments.

for potential human and ecological toxicity.^{2,3} PFAS has shown toxicological properties against environmental soil microbes, including negative effects on soil respiration and soil bacteria enzyme activity.⁴ Also, when a soil microbial community was exposed to perfluorooctanoic acid (PFOA), the growth of soil microbes was reduced; however, the negative effects were somewhat temporary, and the community recovered within a year.⁵

Conversely, microbial degradation of PFAS is considered one of the most desirable remediation strategies due to the advantages of lower capital and operational costs than abiotic methods.^{6,7} Many recent studies have attempted to find organisms from high PFAS concentration effluent streams that utilize PFAS as a potential carbon source for growth.⁸ However, due to the strength of C–F bonds, PFAS are not nearly as attractive for bacteria to utilize as a carbon source compared to others, such as sugars or lignocellulosic biomass, and there is no known enzymatic pathway which utilizes it as an energy source.⁹ However, several “proof-of-concept” studies have demonstrated the potential of certain microbial species to degrade PFAS. These include *Acidimicrobium* sp. strain A6,¹⁰ dehalogenase possessing strains such as *Dechloromonas* sp. CZR5,¹¹ and various *Pseudomonas* species, such as *Pseudomonas parafulva*.^{12,13}

1. Introduction

Per- and polyfluoroalkyl substances (PFAS) are a group of >10 000 fluorinated synthetic compounds that are highly toxic and environmentally persistent. These compounds are difficult to break down due to the high energy C–F bonds.¹ This leaves a large PFAS accumulation in our soil and water resources and raises concerns

^aDepartment of Chemical and Biomolecular Engineering, University of Nebraska-Lincoln, Lincoln, NE 68510, USA. E-mail: rsaha2@unl.edu

^bDepartment of Civil and Environmental Engineering, University of Nebraska-Lincoln, Lincoln, NE 68588, USA. E-mail: nirupam.aich@unl.edu

^cDepartment of Civil, Structural and Environmental Engineering, University at Buffalo, The State University of New York, Buffalo, NY 14260, USA

† Electronic supplementary information (ESI) available. See DOI: <https://doi.org/10.1039/d5va00106d>

‡ These authors have contributed equally to this work and share the first authorship.



Rhodospseudomonas palustris (hereafter, *R. palustris*) is a highly adaptive Gram-negative, non-sulfur bacterium that can be found in diverse environmental media, such as soil, aquatic sediment, eutrophic ponds,¹⁴ animal waste lagoons,¹⁵ and wastewater.¹⁶ *R. palustris* is known for its high environmental hardiness, resisting the toxicological effects of high metal concentrations, and even removing them under these conditions.^{17,18} Furthermore, *R. palustris* is noteworthy for its ability to break down recalcitrant carbon sources such as lignin breakdown products.^{19–21} This strain also possesses a fluoroacetate dehalogenase (*rpa1163*) enzyme. When purified from bacteria (not *R. palustris*), this enzyme has been observed to cleave the very strong C–F bond from fluoroacetate²² and 2,3,3,3-tetrafluoropropionic acid.²³ To assess the potential of *R. palustris* for PFAS biodegradation, it is crucial to study its interactions with PFAS and directly evaluate the toxic effects of these compounds on its morphology and metabolic processes. Therefore, this study aims to pave the road for future PFAS bioremediation studies involving *R. palustris* and Gram-negative bacteria in general by characterizing *R. palustris*' growth and adaptive capabilities when exposed to PFOA as well as PFOA uptake and toxicity to this organism.

2. Methodology

To achieve our above-mentioned objectives, we first conducted a 50-day growth study for *R. palustris* in a photosynthetic media (PM) with exposure to 50 ppm PFOA under anaerobic conditions. The setup consisted of a triplicate control group (lysed cells) and a sample group (live cells). The toxicity effects of PFOA were evaluated by monitoring time dependent bacterial growth through optical density measurements at 660 nm (OD_{660})^{24,25} and by assessing physical cell damage *via* transmission electron microscopy (TEM) imaging.^{26,27} The PFOA uptake by *R. palustris* was evaluated by measuring changes in PFOA concentration in PM at different time intervals using liquid chromatography coupled with tandem mass spectrometry (LC-MS/MS). The underlying mechanisms for uptake *via* cell membranes were further explored *via* surface charge measurements of *R. palustris* cells using a Zetasizer^{26,28} and anion concentration analysis in PM using ion chromatography (IC). Moreover, a 5-day dose-dependent toxicity assay was performed using PM spiked with PFOA concentrations ranging from ~0.78 to 200 ppm, and *R. palustris* growth was measured using OD_{660} . Detailed descriptions of the methodology are provided in the ESI (Section 1).[†]

3. Results and discussion

3.1. PFOA uptake by *R. palustris*

Fig. 1 presents the trend of PFOA uptake from the PFOA-spiked PM containing lysed (control) and live (sample) cell cultures. The PFOA concentration on day 0 was less than the desired 50 ppm initial concentration for both the live samples (36.14 ± 5.00 ppm) and lysed control groups (23.99 ± 2.57 ppm). However, no degradation products were detected from the aliquots collected on day 0. A prior check was performed by preparing 50 ppm PFOA spiked PM without any culture and

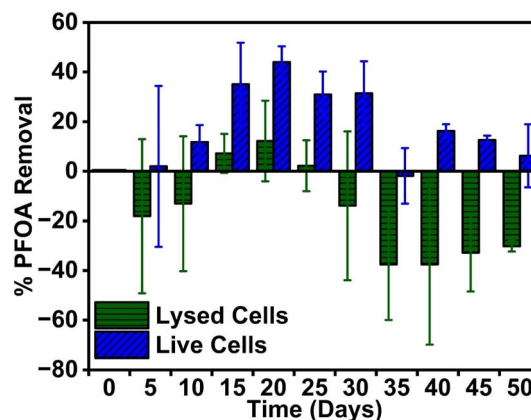


Fig. 1 PFOA removal trends in lysed and live *R. palustris* cells grown in a 50 ppm PFOA spiked PM over 50 days. Error bars represent one standard deviation for $n = 3$ samples.

analyzed similarly to the aliquots from the actual experiment. This check reliably returned concentrations of 44 ± 1.83 ppm, close to 50 ppm. Therefore, the discrepancy observed on day 0 is attributed to the combination of the complex mixture (culture presence in PM) and the potential adsorption on the glass container used for the anaerobic reactor. While using additional controls such as glass containers with PFOA-spiked PM containing no cells is recommended for future bioremediation studies to verify the consumption of PFOA, previous studies have also demonstrated that long-term interaction of PFOA with borosilicate glass led to negligible adsorption.^{29–31} Henceforth in this study, the PFOA concentration values of the live and lysed groups measured on day 0, 36.14 ± 5.00 ppm and 23.99 ± 2.57 ppm, respectively, were used as the initial PFOA concentration in PM on day 0 (C_0) to determine removal capacity (eqn (S1)[†]). In the live sample group, the PFOA removal percentage initially increased gradually to $44 \pm 6.34\%$ until day 20, stabilized from day 20–30, and then showed a significant decrease to $6.23 \pm 12.75\%$ by day 50 ($p < 0.05$, Table S2[†]). In the lysed group, PFOA levels increased from 23.98 ± 2.57 ppm on day 0 to 28.02 ± 5.80 ppm on day 5 and reached 26.67 ± 4.00 ppm on day 10. This increase might be attributed to the initial adsorption of PFOA onto lysed cells *via* hydrophobic interactions, followed by the release of adsorbed PFOA due to structural degradation of autoclaved cell membranes over time. However, PFOA removal reached $12.19 \pm 16.30\%$ on day 20 for the lysed group, with final concentrations at 50 days showing no net uptake by the lysed cells. Statistical analysis for the lysed group showed no significant change in removal from day 0 to day 50 concentration ($p > 0.05$, Table S2[†]). This indicated PFOA uptake was happening in the presence of live culture. A similar observation has been reported for two *Pseudomonas* sp. strains, where the release of perfluorohexane sulfonate (PFHxS) occurred after 15 days of incubation.²⁷ Another Gram-negative, photosynthetic bacterium, *Synechocystis* PCC 6803, has also been reported to release perfluorooctane sulfonate (PFOS) fractionally due to cell lysis.³²

The significant difference in the PFOA removal percentage between the live and lysed bacteria during days 15–45 indicates



that more PFOA is uptaken by live *R. palustris* cells than by lysed ones ($p < 0.05$, Table S2†). The gradual increase in PFOA uptake (until day 20) and release in later days might be a result of a complex interaction process that includes physical hydrophobic and electrostatic interactions, along with biological ion transport mechanisms. The uptaken PFOA might be incorporated into the phospholipid bilayer of the cell membrane, likely due to hydrophobic interaction.²⁸ Additionally, the presence of various proteins on the cell membrane and the proteinophilicity of PFAS compounds might also facilitate PFOA uptake.³³ The PFOA decrease in PM might be due to physical PFOA adsorption on the outer cell surface and its incorporation into the cell. When suspended in deionized (DI) water, the live and lysed *R. palustris* cells from day 20 have shown high negative charges of -36.9 ± 0.977 mV and -43.9 ± 0.912 mV, respectively (Fig. S2.1†). As both PFOA and *R. palustris* have high negative surface charges, electrostatic repulsion would hinder the adsorption of PFOA on the cells. However, the high ion concentrations (calculated to be 189.42 mM) in the PFOA-spiked PM reduced the surface charges to -9.31 ± 0.83 mV and -14.2 ± 0.625 mV for the live and lysed cell cultures, respectively (Fig. S2.1†). This would allow PFOA to be near the cells and partition to cell membranes driven by hydrophobicity. Throughout the 50-day experiment, live bacteria cells had uptaken more PFOA than lysed cells. This is because a higher negative surface charge on the lysed bacteria would result in stronger electrostatic repulsion between PFOA and the lysed cell than the live ones. While active ion transport in live bacteria might also facilitate PFOA uptake, the absence of functional ion transport mechanisms in lysed cells prevented PFOA uptake. Moreover, due to inactive ion transport and damaged cell membranes, charged molecules might leak from within the lysed cell and accumulate on the cell surface.³⁴ This would explain the lysed cells having more negative surface charge than live bacteria, a finding consistent with other studies.^{34,35} Furthermore, bacterial growth in the live group might increase biomass content over time compared to the lysed group, contributing to higher PFOA removal by live bacteria than the lysed ones. Cell lysis might be responsible for the eventual partial release of the incorporated PFOA.³²

3.2. Free anion mass balance in PM

Since day 20 exhibited the highest PFOA removal (Fig. 1), the live group PM was further analyzed to determine possible nutrient consumption and identify other anion generation, such as fluoride (F^-). IC results showed 90.01 ± 7.64 ppm chloride, 3051.30 ± 242.62 ppm phosphate, and 2279.56 ± 214.84 ppm sulfate in the PM at day 20 (Fig. S2.2†). While the chloride and sulfate concentrations remained constant in the PM, the phosphate concentration decreased 67.87% from the initial concentration of 9497 ppm. As phosphate acts as a crucial nutrient for cell development and function in *R. palustris*, the decrease in phosphate amount over 20 days indicated the growth of *R. palustris* in PFOA spiked PM.^{15,36} However, no fluoride ion was detected in the PM, indicating that the PFOA uptaken by the microbe had only been stored in the cells and not metabolized. While the ions

available in the PM media are essential for bacterial growth and assist sorption by reducing electrostatic repulsion between PFOA and cell surface, the extensive effect of high ionic strength and ionic composition on the PFOA sorption capability of bacteria remains unclear.³³ Furthermore, high ion concentrations have been observed to significantly reduce the critical micelle concentration (CMC) of PFAS compounds.^{37,38} PFOA has a high CMC value of 10 350 ppm (~ 26 mM).^{39,40} However, hemi-micelle formation on a solid surface is feasible at concentrations 0.001–0.01 times the CMC.⁴¹ As the starting PFOA concentration (50 ppm or 0.12 mM) in this experiment was within the feasibility limit (0.025–0.25 mM), some hemi-micelles might have formed *via* the attachment of the hydrophobic tail of PFOA on the cell surface. The formation of aggregated PFOA molecules on the cell surface would reduce the amount of free PFOA molecules in the PM. Hence, high ion concentration in PM might positively affect bacteria's sorption capacity and lower bioavailability. In wastewater treatment systems, the ionic strength of streams ranges from 3–100 mM, highlighting the need for further research into the suitability of *R. palustris* for integration into these environments.

3.3. *R. palustris* growth under PFOA exposure

To observe the effects of PFOA on the growth of *R. palustris*, OD_{660} was measured every sampling day (Fig. S2.3a†). Ideally, this would have produced a curve where the growth of *R. palustris* cultures exposed to PFOA would be either identical to or slightly higher than the control acetate curves. However, wild type *R. palustris* exhibits significantly slower growth when exposed to PFAS than when exposed to acetate. An anaerobic wild type *R. palustris* culture (without PFAS) would typically take 3–5 days to reach a maximum OD_{660} of roughly 0.6 (Fig. S2.3b†),^{20,42,43} whereas our PFOA-exposed live cultures grew at an incredibly slow rate, taking 45 days to reach the same maximum OD_{660} . As our experiment allowed for continuous growth by supplementation of 2 mM sodium acetate every 5th day, the reduced max OD_{660} and slower growth rate strongly suggest that our cultures are continuously experiencing cell lysis from the toxicological effects of PFOA. A second noticeable trend we observed was an initial, large, albeit temporary, increase in OD_{660} and the presence of two growth phases, or diauxic growth (before and after day 10). This type of growth usually occurs in cultures with two carbon sources, where an organism preferentially consumes one over the other.^{44–46} However, due to the lack of fluoride present in the media after growth and the inconsistent PFOA mass balance, this might instead be the result of an adaptive phase, where *R. palustris* responds to PFOA exposure. The apparent accelerated death phase might then be explained by cell lysis before *R. palustris* has fully adapted. pH change was also trivial for the duration of the experiment, owing to the high amount of phosphate present in the media (Fig. S2.4†).

3.4. PFOA effect on *R. palustris* morphology

To further evaluate the toxic effects of PFOA, the TEM images (Fig. S2.5†) provided additional information on the live cell



structure and growth in the presence and absence of PFOA. Healthy wild type *R. palustris* cell cultures without PFOA exposure were observed to contain nucleoid and smooth cell membranes (Fig. S2.5a & b†). However, the high-magnification images showed PFOA-exposed live cells from days 0, 20, and 35 with visible damages from possible oxidative stress, such as the absence of nucleoids, cytoplasm leakage,^{47–49} detached cytoplasm from cell wall,⁵⁰ cell wall disruption,^{50–52} and uneven cell membranes (Fig. S2.5d, f, & h†).⁵¹ Similar damages in different bacterial cells from PFAS exposure have been reported in other works.^{27,53} Due to the consistency in TEM imagery between these studies involving metal oxides, chitosan, and PFOA, cell lysis may be caused by these mechanisms.⁵⁴ Even with these toxic effects, the low-magnification images (Fig. S2.5b, e, & g†) showed an increasing number of live cells from day 0 to 35 under PFOA exposure. This corroborated with the growth curve (Fig. S2.3†), indicating the ability of *R. palustris* to grow in the presence of a high concentration of PFOA (*i.e.*, 50 ppm).

3.5. Dose-dependent toxicity assay

Given the irregular growth and morphological damage observed in our initial 50 ppm experiment, a 5-day dose-dependent toxicity assay was performed, in which wild-type *R. palustris* was incubated with a gradient of PFOA concentrations. The purpose of this experiment was to reproduce the irregular growth profile observed in the 50 ppm concentration cultures and to assess whether this effect also exists or is amplified at other PFOA concentrations. A 2× series dilution of PFOA supplemented PM media, ranging from final concentrations of 200 ppm to ~0.78 ppm, was prepared, as well as a control media containing no PFOA (Fig. 2). 3 replicates of 500 μL anaerobic *R. palustris* cultures were then prepared with each individual PFOA concentration, and growth was measured every 12 hours. From our results, two very interesting trends emerge; firstly, the initial large temporary increase in OD₆₆₀, which occurs in the first 24 hours, is present for PFOA concentrations above 12.5 ppm. This effect begins at 12.5 ppm and increases in intensity until 100 ppm, where higher concentrations almost completely

inhibit sustained *R. palustris* growth. Only the 0.78 ppm culture produces no significant difference at any point during growth, while concentrations 12.5 ppm and above produce significantly ($p < 0.05$) reduced growth after 24 hours (Table S3†). Secondly, these cultures appear to emulate diauxic growth behavior. However, considering the lack of PFOA degradation as observed from our mass balance and IC results, we hypothesize that this may be a period during which *R. palustris* responds to the toxicological effects of PFOA. To the best of our knowledge, no existing literature reports a growth pattern similar to the one we have observed. This could imply a unique resistance or adaptation mechanism that *R. palustris* possesses, allowing it to grow even in very high PFOA concentrations. A recent study demonstrated the ability of PFOA to incorporate itself into lipid bilayers up to a saturation limit, thereby expanding the bilayer and increasing membrane fluidity.⁵⁵ Other studies also list membrane disruption, alongside oxidative stress and DNA damage, as potential sources of cell lysis.^{26,56} Due to the similarity in image mechanisms, we hypothesize that the toxicity gradient we observed results from this phenomenon, where PFOA is saturating the cell membrane until it is ruptured. However, the underlying mechanism of *R. palustris* to effectively respond to and recover from this toxicological effect remains to be understood.

4. Conclusions

In summary, this study presents the potential of *R. palustris* for PFOA removal and elucidates the microbes' unique adaptation pattern to the toxic effects of PFOA. At a high PFOA concentration of 50 ppm, *R. palustris* temporarily removed PFOA from the surrounding media either by incorporation into or adsorption on the cell membrane. While the PFOA removal reached a maximum uptake of ~44% after 20 days, eventual PFOA release happens from the cell membrane. The full toxicity range of PFOA on *R. palustris* is determined, where cultures exposed to ~0.78 ppm of PFOA are identical to cultures grown without PFOA. The growth inhibition increases with increasing PFOA concentration and is almost completely inhibited at 200 ppm. *R. palustris* also exhibits interesting growth adaptation behavior, where an initial growth phase is followed by an accelerated death phase due to the high concentration of PFOA. Another growth phase follows when *R. palustris* cultures are supplemented with 12.5–100 ppm PFOA. This study demonstrates that a PFOA concentration ceiling limit exists for effective bioremediation; beyond that, *R. palustris* suffers severe toxicity effects. While no degradation product or fluoride generation was observed in this study, this strain has previously demonstrated the ability to degrade other halogenated compounds at much lower concentrations.⁵⁷ Instead of showing evidence of degradation, *R. palustris* appears to simply uptake PFOA at this high concentration. Hence, further research is needed to optimize the growth conditions and establish an environment conducive to enzymatic activity. Along with this, we plan to perform non-targeted mass spectroscopy analysis to identify if any unknown transformation products formed during this period of PFOA exposure to *R. palustris* in future studies. Although further

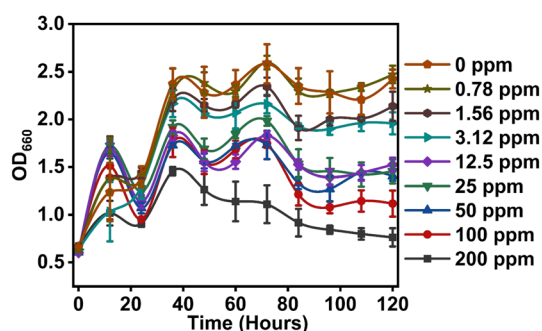


Fig. 2 Wild type *R. palustris* grown on a 2× serial dilution of PFOA (200–0.78 ppm) over 5 days. The growth curves exhibited an accelerated death phase in the initial hours (12–24 hours) for the PFOA concentrations of 12.5–200 ppm. With increasing PFOA concentrations, the maximum OD₆₆₀ decreases. Error bars represent one standard deviation for $n = 3$ samples.



work is required to evaluate the bioremediation potential of *R. palustris* extensively, the results presented here provide groundwork on understanding the behavior of *R. palustris* and similar Gram-negative bacteria in PFOA-contaminated media.

Data availability

All data needed to evaluate the conclusions in the paper are present in the paper and/or the ESI.†

Conflicts of interest

There are no conflicts to declare.

Acknowledgements

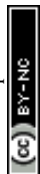
This work was supported by the University of Nebraska-Lincoln Layman Seed Grant and Nebraska Collaboration Initiative Grant awarded to R. S. and N. A. This work was also supported by the National Science Foundation CAREER Grant (1943310) awarded to R. S. This work was partially supported by National Science Foundation Grant (2324853) awarded to N. A. The research was partially performed at the UNL Nebraska Center for Biotechnology. We thank Dr You Zhou and Dr Bara Altartouri from the NCB Microscopy Core Research Facility for their assistance with the TEM sample preparation and imaging.

References

- H. Son, T. Kim, H.-S. Yoom, D. Zhao and B. An, The Adsorption Selectivity of Short and Long Per- and Polyfluoroalkyl Substances (PFASs) from Surface Water Using Powder-Activated Carbon, *Water*, 2020, **12**(11), 3287.
- G. M. Sinclair, S. M. Long and O. A. H. Jones, What are the effects of PFAS exposure at environmentally relevant concentrations?, *Chemosphere*, 2020, **258**, 127340.
- Y. Wang, U. Munir and Q. Huang, Occurrence of per- and polyfluoroalkyl substances (PFAS) in soil: Sources, fate, and remediation, *Soil Environ. Health*, 2023, **1**(1), 100004.
- B. Xu, G. Yang, A. Lehmann, S. Riedel and M. C. Rillig, Effects of perfluoroalkyl and polyfluoroalkyl substances (PFAS) on soil structure and function, *Soil Ecol. Lett.*, 2023, **5**(1), 108–117.
- R. Xu, W. Tao, H. Lin, D. Huang, P. Su, P. Gao, *et al.*, Effects of Perfluorooctanoic Acid (PFOA) and Perfluorooctane Sulfonic Acid (PFOS) on Soil Microbial Community, *Microb. Ecol.*, 2022, **83**(4), 929–941.
- Z. Zhang, D. Sarkar, J. K. Biswas and R. Datta, Biodegradation of per- and polyfluoroalkyl substances (PFAS): A review, *Bioresour. Technol.*, 2022, **344**, 126223.
- E. Shahsavari, D. Rouch, L. S. Khudur, D. Thomas, A. Aburto-Medina and A. S. Ball, Challenges and Current Status of the Biological Treatment of PFAS-Contaminated Soils, *Front. Bioeng. Biotechnol.*, 2021, **8**, 602040.
- M. Marciesky, D. S. Aga, I. M. Bradley, N. Aich and C. Ng, Mechanisms and Opportunities for Rational In Silico Design of Enzymes to Degrade Per- and Polyfluoroalkyl Substances (PFAS), *J. Chem. Inf. Model.*, 2023, **63**(23), 7299–7319.
- D. B. Harper, D. O'Hagan and C. D. Murphy, Fluorinated Natural Products: Occurrence and Biosynthesis, in *Natural Production of Organohalogen Compounds*, ed. Gribble G., Springer Berlin Heidelberg, Berlin, Heidelberg, 2003, pp. 141–169.
- M. Ruiz-Urigüen, W. Shuai, S. Huang and P. R. Jaffé, Biodegradation of PFOA in microbial electrolysis cells by Acidimicrobiaceae sp. strain A6, *Chemosphere*, 2022, **292**, 133506.
- M. Long, C. W. Zheng, M. A. Roldan, C. Zhou and B. E. Rittmann, Co-Removal of Perfluorooctanoic Acid and Nitrate from Water by Coupling Pd Catalysis with Enzymatic Biotransformation, *Environ. Sci. Technol.*, 2024, **58**(26), 11514–11524.
- L. B. Yi, L. Y. Chai, Y. Xie, Q. J. Peng and Q. Z. Peng, Isolation, identification, and degradation performance of a PFOA-degrading strain, *Genet. Mol. Res.*, 2016, **15**(2), 15028043.
- L. Yi, Q. Peng, D. Liu, L. Zhou, C. Tang, Y. Zhou, *et al.*, Enhanced degradation of perfluorooctanoic acid by a genome shuffling-modified *Pseudomonas parafulva* YAB-1, *Environ. Technol.*, 2019, **40**(24), 3153–3161.
- A. Rayyan, T. Meyer and J. Kyndt, Draft Whole-Genome Sequence of the Purple Photosynthetic Bacterium *Rhodospseudomonas palustris* XCP, *Microbiol. Resour. Announce.*, 2018, **7**(4), e00855.
- M. K. Kim, K. M. Choi, C. R. Yin, K. Y. Lee, W. T. Im, J. H. Lim, *et al.*, Odorous swine wastewater treatment by purple non-sulfur bacteria, *Rhodospseudomonas palustris*, isolated from eutrophicated ponds, *Biotechnol. Lett.*, 2004, **26**(10), 819–822.
- C. S. Harwood, *Rhodospseudomonas palustris*, *Trends Microbiol.*, 2022, **30**(3), 307–308.
- I. Llorens, G. Untereiner, D. Jaillard, B. Gouget, V. Chapon and M. Carriere, Uranium Interaction with Two Multi-Resistant Environmental Bacteria: *Cupriavidus metallidurans* CH34 and *Rhodospseudomonas palustris*, *PLoS One*, 2012, **7**(12), e51783.
- C. Zhao, Y. Zhang, Z. Chan, S. Chen and S. Yang, Insights into arsenic multi-operons expression and resistance mechanisms in *Rhodospseudomonas palustris* CGA009, *Front. Microbiol.*, 2015, **6**, 180.
- C. S. Harwood and J. Gibson, Anaerobic and aerobic metabolism of diverse aromatic compounds by the photosynthetic bacterium *Rhodospseudomonas palustris*, *Appl. Environ. Microbiol.*, 1988, **54**(3), 712–717.
- B. Brown, C. Immethun, A. Alsiyabi, D. Long, M. Wilkins and R. Saha, Heterologous phasin expression in *Rhodospseudomonas palustris* CGA009 for bioplastic production from lignocellulosic biomass, *Metab. Eng. Commun.*, 2022, **14**, e00191.
- A. Alsiyabi, B. Brown, C. Immethun, D. Long, M. Wilkins and R. Saha, Synergistic experimental and computational approach identifies novel strategies for polyhydroxybutyrate overproduction, *Metab. Eng.*, 2021, **68**, 1–13.



- 22 W. Y. Chan, M. Wong, J. Guthrie, A. V. Savchenko, A. F. Yakunin, E. F. Pai, *et al.*, Sequence- and activity-based screening of microbial genomes for novel dehalogenases, *Microb. Biotechnol.*, 2010, **3**(1), 107–120.
- 23 Y. Li, Y. Yue, H. Zhang, Z. Yang, H. Wang, S. Tian, *et al.*, Harnessing fluoroacetate dehalogenase for defluorination of fluorocarboxylic acids: in silico and in vitro approach, *Environ. Int.*, 2019, **131**, 104999.
- 24 M. Kathol, C. Immethun and R. Saha, Protocol to develop a synthetic biology toolkit for the non-model bacterium *R. palustris*, *STAR Protoc.*, 2023, **4**(2), 102158.
- 25 A. Govindaraju, J. B. McKinlay and B. LaSarre, Phototrophic Lactate Utilization by *Rhodospseudomonas palustris* Is Stimulated by Co-utilization with Additional Substrates, *Appl. Environ. Microbiol.*, 2019, **85**(11), e00048.
- 26 G. Liu, S. Zhang, K. Yang, L. Zhu and D. Lin, Toxicity of perfluorooctane sulfonate and perfluorooctanoic acid to *Escherichia coli*: Membrane disruption, oxidative stress, and DNA damage induced cell inactivation and/or death, *Environ. Pollut.*, 2016, **214**, 806–815.
- 27 A. Presentato, S. Lampis, A. Vantini, F. Manea, F. Daprà, S. Zuccoli, *et al.*, On the Ability of Perfluorohexane Sulfonate (PFHxS) Bioaccumulation by Two *Pseudomonas* sp. Strains Isolated from PFAS-Contaminated Environmental Matrices, *Microorganisms*, 2020, **8**(1), 92.
- 28 N. J. M. Fitzgerald, A. Wargenau, C. Sorenson, J. Pedersen, N. Tufenkji, P. J. Novak, *et al.*, Partitioning and Accumulation of Perfluoroalkyl Substances in Model Lipid Bilayers and Bacteria, *Environ. Sci. Technol.*, 2018, **52**(18), 10433–10440.
- 29 J. Cao and F. Xiao, Interactions of per- and polyfluoroalkyl substances with polypropylene plastic and borosilicate glass: Resolving key uncertainties for accurate analysis, *J. Hazard. Mater. Adv.*, 2024, **16**, 100463.
- 30 S. Lath, E. R. Knight, D. A. Navarro, R. S. Kookana and M. J. McLaughlin, Sorption of PFOA onto different laboratory materials: Filter membranes and centrifuge tubes, *Chemosphere*, 2019, **222**, 671–678.
- 31 J. E. Zenobio, O. A. Salawu, Z. Han and A. S. Adeleye, Adsorption of per- and polyfluoroalkyl substances (PFAS) to containers, *J. Hazard. Mater. Adv.*, 2022, **7**, 100130.
- 32 F. Marchetto, M. Roverso, D. Righetti, S. Bogialli, F. Filippini, E. Bergantino, *et al.*, Bioremediation of Per- and Poly-Fluoroalkyl Substances (PFAS) by *Synechocystis* sp. PCC 6803: A Chassis for a Synthetic Biology Approach, *Life*, 2021, **11**(12), 1300.
- 33 M. Dai, N. Yan and M. L. Brusseau, Potential impact of bacteria on the transport of PFAS in porous media, *Water Res.*, 2023, **243**, 120350.
- 34 C. Ayala-Torres, N. Hernández, A. Galeano, L. Novoa-Aponte and C.-Y. Soto, Zeta potential as a measure of the surface charge of mycobacterial cells, *Ann. Microbiol.*, 2014, **64**(3), 1189–1195.
- 35 R. E. Martinez, O. S. Pokrovsky, J. Schott and E. H. Oelkers, Surface charge and zeta-potential of metabolically active and dead cyanobacteria, *J. Colloid Interface Sci.*, 2008, **323**(2), 317–325.
- 36 C. Berne, B. Allainmat and D. Garcia, Tributyl phosphate degradation by *Rhodospseudomonas palustris* and other photosynthetic bacteria, *Biotechnol. Lett.*, 2005, **27**(8), 561–566.
- 37 N. Downes, G. A. Ottewill and R. H. Ottewill, An investigation of the behaviour of ammonium perfluoro-octanoate at the air/water interface in the absence and presence of salts, *Colloids Surf., A*, 1995, **102**, 203–211.
- 38 S. Kancharla, R. Jahan, D. Bedrov, M. Tsianou and P. Alexandridis, Role of chain length and electrolyte on the micellization of anionic fluorinated surfactants in water, *Colloids Surf., A*, 2021, **628**, 127313.
- 39 T. Sahara, D. Wongsawaeng, K. Ngaosuwan, W. Kiatkittipong, P. Hosemann and S. Assabumrungrat, Highly effective removal of perfluorooctanoic acid (PFOA) in water with DBD-plasma-enhanced rice husks, *Sci. Rep.*, 2023, **13**(1), 13210.
- 40 S. Kancharla, D. Dong, D. Bedrov, M. Tsianou and P. Alexandridis, Structure and Interactions in Perfluorooctanoate Micellar Solutions Revealed by Small-Angle Neutron Scattering and Molecular Dynamics Simulations Studies: Effect of Urea, *Langmuir*, 2021, **37**(17), 5339–5347.
- 41 R. P. Schwarzenbach, P. M. Gschwend and D. M. Imboden, *Environmental Organic Chemistry*, John Wiley & Sons, New York, 2nd edn, 2003.
- 42 C. M. Immethun, M. Kathol, T. Changa and R. Saha, Synthetic Biology Tool Development Advances Predictable Gene Expression in the Metabolically Versatile Soil Bacterium *Rhodospseudomonas palustris*, *Front. Bioeng. Biotechnol.*, 2022, **10**, DOI: [10.3389/fbioe.2022.800734](https://doi.org/10.3389/fbioe.2022.800734).
- 43 B. Brown, C. Immethun, M. Wilkins and R. Saha, *Rhodospseudomonas palustris* CGA009 polyhydroxybutyrate production from a lignin aromatic and quantification via flow cytometry, *Bioresour. Technol. Rep.*, 2020, **11**, 100474.
- 44 N. A. Tyrovouzis, A. S. Angelidis and N. G. Stoforos, Bi-phasic growth of *Listeria monocytogenes* in chemically defined medium at low temperatures, *Int. J. Food Microbiol.*, 2014, **186**, 110–119.
- 45 H. Sun, X. Zhang, D. Wang and Z. Lin, Insights into the role of energy source in hormesis through diauxic growth of bacteria in mixed cultivation systems, *Chemosphere*, 2020, **261**, 127669.
- 46 R. Mahadevan, J. S. Edwards and F. J. Doyle 3rd, Dynamic flux balance analysis of diauxic growth in *Escherichia coli*, *Biophys. J.*, 2002, **83**(3), 1331–1340.
- 47 L. Moreira, N. M. Guimarães, S. Pereira, R. S. Santos, J. A. Loureiro, M. C. Pereira, *et al.*, Liposome Delivery of Nucleic Acids in Bacteria: Toward In Vivo Labeling of Human Microbiota, *ACS Infect. Dis.*, 2022, **8**(7), 1218–1230.
- 48 I. Lopez-Heras, I. Theodorou, B. Ley, M. Ryan and A. Porter, Towards Understanding the Antibacterial Activity of Ag Nanoparticles: Electron microscopy in the analysis of the materials-biology interface in the lung, *Environ. Sci.: Nano*, 2015, **2**, DOI: [10.1039/C5EN00051C](https://doi.org/10.1039/C5EN00051C).
- 49 M. Schulte, M. Hensel, and K. Miskiewicz, Exposure to stressors and antimicrobials induces cell-autonomous



- ultrastructural heterogeneity of an intracellular bacterial pathogen, *bioRxiv*, 2020, preprint, 2020.09.14.297432, DOI: [10.1101/2020.09.14.297432](https://doi.org/10.1101/2020.09.14.297432).
- 50 A. H. Phakatkar, F. Emre, A. Laura, S. Boao, N. Surya, R. Ramin, *et al.*, TEM Studies on Antibacterial Mechanisms of Black Phosphorous Nanosheets, *Int. J. Nanomed.*, 2020, **15**, 3071–3085.
- 51 J. Kuang, Y. Lin, L. Wang, Z. Yan, J. Wei, J. Du, *et al.*, Effects of PEF on Cell and Transcriptomic of *Escherichia coli*, *Microorganisms*, 2024, **12**(7), 1380.
- 52 Y. Ding, G. Wen, X. Wei, H. Zhou, C. Li, Z. Luo, *et al.*, Antibacterial activity and mechanism of luteolin isolated from *Lophatherum gracile* Brongn. against multidrug-resistant *Escherichia coli*, *Front. Pharmacol.*, 2024, **15**, 1430564.
- 53 A. E. Lindell, A. Griebhammer, L. Michaelis, D. Papagiannidis, H. Ochner, S. Kamrad, *et al.*, Extensive PFAS accumulation by human gut bacteria, *bioRxiv*, 2024, preprint, 2024.09.17.613493, DOI: [10.1101/2024.09.17.613493](https://doi.org/10.1101/2024.09.17.613493).
- 54 J. Li and S. Zhuang, Antibacterial activity of chitosan and its derivatives and their interaction mechanism with bacteria: Current state and perspectives, *Eur. Polym. J.*, 2020, **138**, 109984.
- 55 T. N. Sobolewski, R. C. Trousdale, C. L. Gauvin, C. M. Lawrence and R. A. Walker, Nanomolar PFOA Concentrations Affect Lipid Membrane Structure: Consequences for Bioconcentration Mechanisms, *Environ. Sci. Technol.*, 2025, **59**(1), 709–718.
- 56 N. J. M. Fitzgerald, M. F. Simcik and P. J. Novak, Perfluoroalkyl Substances Increase the Membrane Permeability and Quorum Sensing Response in *Aliivibrio fischeri*, *Environ. Sci. Technol. Lett.*, 2018, **5**(1), 26–31.
- 57 Y.-J. Li, R. Wang, C.-Y. Lin, S.-H. Chen, C.-H. Chuang, T.-H. Chou, *et al.*, The degradation mechanisms of *Rhodopseudomonas palustris* toward hexabromocyclododecane by time-course transcriptome analysis, *Chem. Eng. J.*, 2021, **425**, 130489.

